

REACTIVE SPECIES DELIVERY IN ATMOSPHERIC He+O₂ COLD PLASMA

A. J. YANG, D. X. LIU, X. H. WANG* AND M. Z. RONG

State Key Lab of Electrical Insulation and Power Equipment, Xi'an Jiaotong University, Xi'an, 710049, P.R. China.

* xhw@mail.xjtu.edu.cn

ABSTRACT

Atmospheric He+O₂ cold plasma, rich in reactive oxygen species(ROS), has attracted a great deal of attention. Much research has focused on the ROS generation in plasmas, but little for delivering of such species out of plasmas. In plasma treatment, the dosage of ROS that can act on the treated target is of great importance, but how to quantify such dosage by simulation is still unknown. Regarding to this, a fluid model of He+O₂ radio-frequency(RF) discharge is developed in this paper, by which the dosage of ROS is quantitatively investigated. It is found that the dosage of ROS is dominated by plasma sheath, because the ROS generated in bulk regime has little probability to be delivered out of plasmas and act on the treated target.

1. INTRODUCTION

In recent years there has been a growing interest on RF atmospheric pressure glow discharge(APGD) due to lower-cost and easier implementation than their low-pressure counterparts^[1, 2]. In many of the envisioned applications of atmospheric pressure plasmas, it is almost impossible to prevent the presence of oxygen in discharge and a very low impurity level can change significantly the plasma chemistry^[3, 4]. Besides, oxygen containing plasmas are rich of reactive species(e.g. atomic oxygen) and have enabled advances in application. As a result, He+O₂ atmospheric pressure plasmas were extensively investigated in the last decade for various applications from material processing to biomedicine^[5-7]. In search for ROS production efficiency, various experimental and numerical studies^[8,9] focusing on He+O₂ atmospheric pressure plasmas have

been done. However, most of the researches have focused on the ROS generation in plasmas, little for delivering of such species out of plasmas. Regarding to this, a fluid model of He+O₂ RF discharge is developed in this paper, by which the dosage of ROS is quantitatively investigated.

2. DESCRIPTION OF THE MODEL

The plasma source system consists of two plane-parallel electrodes with a narrow separation of 2mm and a large electrode width. The electrode width is much larger than the electrode gap to allow for a one-dimensional model. The fluid model solves the mass conservation equation for each species, the current continuity equation and the electron energy conservation equation. Given the high collisionality of the discharge, the particles inertia is neglected and the drift-diffusion approximation is used in the model. A detailed description of the set of equations and boundary conditions can be found in our previous study^[10,11,12] references therein. The feedstock gas is helium with impurity of oxygen. The fraction of oxygen is 5000ppm. The species and reactions considered in the model are selected from detailed global model simulations^[4]. The transport coefficients for all species are obtained from Ref.10 and references therein. The power density is set to be 40Wcm⁻³. It is assumed that the gas temperature is 350 K and the secondary electron emission coefficient is 0.01.

3. RESULTS AND DISCUSSIONS

Since a sheath forms above an electrode or a sample inserted into the plasma, fluxes arriving at one electrode may be used as fluxes arriving at the inserted sample. To this end, wall flux is

used here as a general term and is exchangeable in its use with the term of electrode flux.

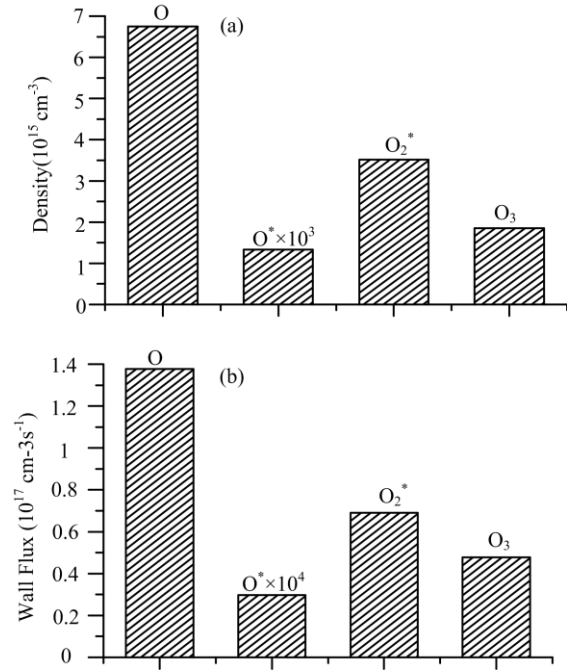


Fig.1 Spatial-temporally averaged (a) and time-averaged wall fluxes(b) of neutral species.

Fig.1 shows the spatial-temporally averaged and time-averaged wall fluxes of neutral species. In the bulk plasma, the flux of a plasma species is given by $\Gamma_k = n_k v_k / 4$ with n_k and v_k being its concentration and its transport velocity, respectively. Therefore, it is of interest to compare the flux ratios of O, O^* , O_2^* and O_3 with their concentration ratios.

For neutral species, it is obvious from Fig.1(a) that ground-state oxygen atom has the largest density at $n_{\text{O}} = 6.7 \times 10^{15} \text{ cm}^{-3}$, followed by excited oxygen molecules ($n_{\text{O}}/n_{\text{O}_2^*} = 1.87$) and ozone ($n_{\text{O}}/n_{\text{O}_3} = 3.62$). By contrast, the density of excited oxygen atoms is more than three orders of magnitude below that of O ($n_{\text{O}}/n_{\text{O}^*} = 5150$). Besides it is also can be seen from Fig.1(b) that ground-state oxygen atom has the largest flux at $\Gamma_{\text{O}} = 1.38 \times 10^{17} \text{ cm}^{-3} \text{ s}^{-1}$, followed by excited oxygen molecules and ozone, similar to their densities. It is interesting that the ratios of Γ_{O} to the wall fluxes of O_2^* and O_3 are $\Gamma_{\text{O}}/\Gamma_{\text{O}_2^*} = 2$ and $\Gamma_{\text{O}}/\Gamma_{\text{O}_3} = 2.89$, almost identical to their corresponding flux ratios. This close correlation suggests that O, O_2^* and O_3 generated in the plasma are transported to an electrode with very similar transportation losses. The relative magnitudes of electrode fluxes are therefore a faithful reflection of their space-averaged

concentrations. By contrast, $\Gamma_{\text{O}}/\Gamma_{\text{O}^*}$ is found to be 47000, about one order of magnitude above $n_{\text{O}}/n_{\text{O}^*}$. This means that O^* suffers much greater loss in its transport to an electrode than all other three reactive neutral species.

It is important to recognize that only plasma species with adequate lifetimes could reach the electrode from the plasma region and hence contribute to their wall fluxes. Effective lifetimes of all four neutral oxygen species are found to be $\tau_{\text{O}} = 1.1 \text{ ms}$, $\tau_{\text{O}_2^*} = 1.25 \text{ ms}$, $\tau_{\text{O}_3} = 1.0 \text{ ms}$ and $\tau_{\text{O}^*} = 0.5 \mu\text{s}$ estimated from relevant rate coefficients^[10] similar to that used previously⁰. Then the lifetimes of neutral species are used to estimate the excursion distance during lifetime (EDL) using $L = \sqrt{D\tau}$ where D is the diffusion coefficient and τ is the effective lifetime. It is found that their EDLs are $L_{\text{O}} = 285 \mu\text{m}$, $L_{\text{O}_2^*} = 284 \mu\text{m}$, $L_{\text{O}_3} = 223 \mu\text{m}$ and $L_{\text{O}^*} = 6 \mu\text{m}$. Our simulation data suggest the cathode sheath thickness is $d_{\text{sh}} = 470 \mu\text{m}$, meaning that the EDL of O, O_2^* and O_3 are about 47-61% of the sheath thickness and $L_{\text{O}^*}/d_{\text{sh}}$ is only 1.2%. Wall flux of any plasma species is supplied by its generation largely within its EDL from the wall, and the resulting loss of its concentration (in supplying the wall flux) needs to be replenished from its generation outside the EDL. For O, O_2^* and O_3 , their EDLs being a significant fraction of the sheath thickness suggest that their wall losses are likely to be fully replenished. This may be responsible for the close correlation observed between the ratios of their wall fluxes (e.g. $\Gamma_{\text{O}}/\Gamma_{\text{O}_2^*}$) to those of their space-averaged concentrations (e.g. $n_{\text{O}}/n_{\text{O}_2^*}$). For excited oxygen atoms, their EDL of only 6 μm suggests that their replenishment is effective only locally over a very short distance, which is the main reason why $\Gamma_{\text{O}^*}/n_{\text{O}^*}$ is much smaller than those of O, O_2^* and O_3 .

Fig.2 illustrates the spatial-temporally averaged and time-averaged wall fluxes of neutral species. As can be seen that the densities of the charged species are almost in the same order and while the wall fluxes of electrons and positive ions are much greater than fluxes of negative ions. Flux ratios of cations (i.e. $\Gamma_{\text{O}_2^+}/\Gamma_{\text{O}_4^+}$) and anions (e.g. $\Gamma_{\text{O}^-}/\Gamma_{\text{O}_2^-}$) are found to correlate numerically to their corresponding concentration ratios (e.g. $n_{\text{O}_2^+}/n_{\text{O}_4^+}$ and $n_{\text{O}^-}/n_{\text{O}_2^-}$) in the sheath region but not those averaged over the entire electrode gap. To understand this, the drift distance of ions is estimated using ion mobility data in ref.10 over a short period during which ion fluxes persist

before the electric field reverses its direction of polarity. For cations, they are driven by a strong electric field near the instantaneous cathode and the drift distances are estimated to be $L_{O_2^+} = 85\mu\text{m}$ and $L_{O_4^+} = 64\mu\text{m}$. It is clear that the drift distances of both cations are shorter than the sheath thickness but nonetheless a large fraction of the latter. Similar to O, O_2^* and O_3 , the large drift distances of $L_{O_2^+}$ and $L_{O_4^+}$ imply that the loss in their concentrations in supplying their wall flux near the instantaneous cathode is likely to be adequately replenished. For anions, their fluxes are driven to the instantaneous anode by a rather weak electric field in the anode sheath and the drift distances of anions are found to be $L_{O^-} = 4.6\mu\text{m}$, $L_{O_2^-} = 3.8\mu\text{m}$ and $L_{O_3^-} = 3.5\mu\text{m}$. Clearly these are markedly smaller than the anode sheath thickness, suggesting a compromised facility to replenish species losses in the anode sheath.

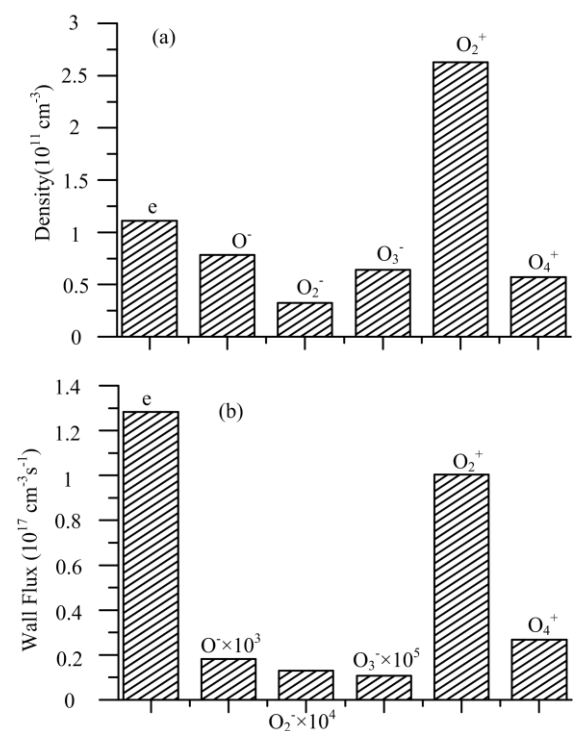


Fig.2 Spatial-temporally averaged (a) and time-averaged wall fluxes (b) of charged species.

From the above discussions, it can be seen that the dose of atmospheric pressure plasmas as experienced by a sample placed on a plasma-facing wall (e.g. an electrode) is supplied from a boundary layer of up to a few hundreds μm in width next to the sample surface rather than from further away within the plasma bulk. The wall fluxes reaching the sample surface are therefore controlled locally by physics and chemistry within the micron-scale boundary layer. In other words, the space-averaged densities are not the

most appropriate indicator of plasma dose experienced by the sample.

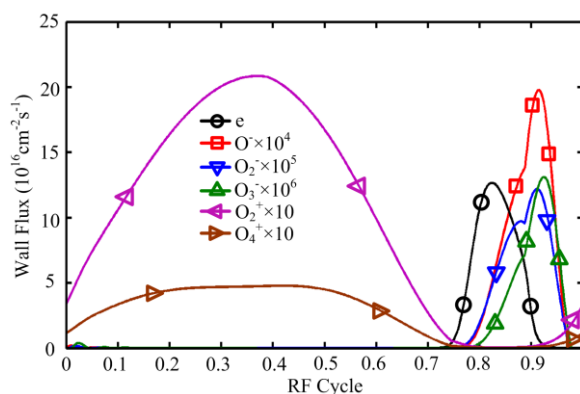


Fig.3 Temporal evolution of electrode fluxes of charged species.

For non-living materials, temporal features of plasma treatment process are of interest usually only in terms of the total treatment as a measure of plasma dose. For materials containing living cells and tissues, the sequence of different plasma species arriving at a sample may be important. To this end, temporal characteristics of wall fluxes are studied.

Fig.3 shows that electrode fluxes of charged particles have a pulse-like form with the anion and electron pulses. There is one pulse every RF period for any type of charged particle. For cations, their movement towards the instantaneous cathode is driven by the sheath electric field and therefore their pulse is formed during the formation of the sheath above the instantaneous cathode. As the cathode sheath is collapsing and the electrode is evolving to become an instantaneous anode, electrons and anions start to move to the electrode. In other words, the pulses of electrons and negative ions are formed after an electrode becomes an instantaneous anode following the collapsing of the cathode sheath in the previous half RF cycle. Electron fluxes are larger than cation fluxes in magnitude but narrower in pulse width, exhibiting a distinct temporal asymmetry. For neutral species, fluxes of O, O_2^* and O_3 vary very little with time and the variation of the O^* flux is at most 10% within one RF period. Taken together the above discussions, a sample treated by an RF atmospheric He+ O_2 plasma is likely to experience a largely time-invariant flux of neutral oxygen species and two alternating pulses of cation and electrons/anion fluxes with asymmetric pulse characteristics.

4. CONCLUSIONS

A 1-D fluid model is developed to study on the reactive species delivery in atmospheric He+O₂ cold plasma. It is found that the dose of atmospheric pressure plasmas as experienced by a sample placed on a plasma-facing wall (e.g. an electrode) is supplied from a boundary layer of up to a few hundreds μm in width next to the sample surface rather than from further away within the plasma bulk. Besides, a sample treated by an RF atmospheric He+O₂ plasma is likely to experience a largely time-invariant flux of neutral oxygen species and two alternating pulses of cation and electrons/anion fluxes with asymmetric pulse characteristics.

ACKNOWLEDGEMENT

This work was supported by the State Key Laboratory of Electrical Insulation and Power Equipment (No.EIPE14312), and National Natural Science Foundation of China (No. 51307134).

REFERENCES

- [1]A. Ladwig, S. Babayan, M. Smith, M. Hester, W. Highland, R. Koch and R. Hicks, "Atmospheric plasma deposition of glass coatings on aluminum", *Surf. Coat. Technol.*, 201, 6460-6464, 2007.
- [2]C. Sarra-Bournet, S. Turgeon, D. Mantovani, and G. Laroche, "Comparison of Atmospheric-Pressure Plasma versus Low-Pressure RF Plasma for Surface Functionalization of PTFE for Biomedical Applications", *Plasma Processes Polym.*, 3, 506-515, 2006.
- [3]D. X. Liu, P. Bruggeman, F. Iza, M. Z. Rong and M. G. Kong, "Global model of low-temperature atmospheric-pressure He+H₂O plasmas", *Plasma Sources Sci. Technol.* 19, 025018, 2010.
- [4]D. X. Liu, M. Z. Rong, X. H. Wang, F. Iza, M. G. Kong and P. Bruggeman, "Main Species and Physicochemical Processes in Cold Atmospheric-pressure He+O₂ Plasmas ", *Plasma Process. Polym.*, 7, 846-865, 2010.
- [5]E. Gonzalez II, M. D. Barankin, P. C. Guschl and R. F. Hicks, "Remote Atmospheric-Pressure Plasma Activation of the Surfaces of Polyethylene Terephthalate and Polyethylene Naphthalate", *Langmuir*, 24, 12636-12643, 2008.
- [6]M. G. Kong, G. Kroesen, G. Morfill, T. Nosenko, T. Shimizu, J. van Dijk and J. L. Zimmermann, "Plasma medicine: an introductory review", *New J. Phys.*, 11, 115012, 2009.
- [7]G. Fridman, A. B. Shekhter, V. N. Vasilets, G. Friedman, A. Gutsol and A. Fridman, "Applied plasma medicine", *Plasma Process. Polym.*, 5, 503, 2008.
- [8]N. Knake, K. Niemi, S. Reuter, V. Schulz-von der Gathen and J. Winter, " Absolute atomic oxygen density profiles in the discharge core of a microscale atmospheric pressure plasma jet", *Appl. Phys. Lett.*, 93, 131503, 2008.
- [9]V. Léveillé and S. Coulombe, " Atomic Oxygen Production and Exploration of Reaction Mechanisms in a He-O₂ Atmospheric Pressure Glow Discharge Torch", *Plasma Process. Polym.*, 3, 587, 2006.
- [10]A. J. Yang, X. H. Wang, M. Z. Rong, D. X. Liu, F. Iza and M. G. Kong, "1-D fluid model of atmospheric-pressure rf He+O₂ cold plasmas: Parametric study and critical evaluation", *Phys. Plasma*, 18, 113503, 2011.
- [11]D. X. Liu, A. J. Yang, X. H. Wang, M. Z. Rong, F. Iza, and M. G. Kong, "Wall fluxes of reactive oxygen species of an rf atmospheric-pressure plasma and their dependence on sheath dynamics", *J. Phys. D: Appl. Phys.*, 45, 305205, 2012.
- [12]A. J. Yang, M. Z. Rong, X. H. Wang, D. X. Liu and M. G. Kong, "Variable radio-frequency cold atmospheric He+O₂ discharges: from electron-heating mechanism to reactive species delivery", *J. Phys. D: Appl. Phys.*, 46, 415201, 2013.
- [13]K. Niemi, J. Waskoenig, N. Sadeghi, T. Gans and D. O'Connell, "The role of helium metastable states in radio-frequency driven helium-oxygen atmospheric pressure plasma jets: measurement and numerical simulation", *Plasma Sources Sci. Technol.*, 20, 055005, 2011.